Geophys. J. R. astr. Soc. (1979) 57, 311–341

Regionalized shear velocity models of the Pacific upper mantle from observed Love and Rayleigh wave dispersion

Guey-Kuen Yu* and Brian J. Mitchell *Department of Earth and Atmospheric Sciences, Saint Louis University, St Louis, Missouri 63156, USA*

Received 1978 May 23

Summary. Group and phase velocities for periods between 16 and 110 s have been determined using the single-station method along 33 Rayleigh- and 30 Love-wave paths across the Pacific. These dispersion data were used to detect variations in upper mantle structure beneath the Pacific. Taking both regional changes and azimuthal anisotropy into consideration, regionalized group and phase velocities were derived for four regions of differing age. The boundaries of the regions were chosen to correspond to isochrons of 20, 50 and 100 Myr, as inferred from geomagnetic lineations. A small, but significant degree of azimuthal anisotropy (less than 0.8 per cent) was found to occur throughout the Pacific if the degree and direction of maximum velocity were assumed to be uniform everywhere. The average direction of maximum velocity was found to be $85^\circ \pm 6^\circ$ as measured clockwise from north. Regionalized group and phase velocities for Rayleigh waves at the larger periods increase systematically with increasing age of the ocean floor. For Love waves, departures from a systematic increase occur in the youngest (0–20 Myr) and oldest (> 100 Myr) portions of the Pacific.

The dispersion data were corrected for the effects of anelasticity and were inverted to obtain shear velocity models for each of the four regions using the stochastic inversion method. A comparison of the shear wave models derived from Rayleigh waves in the four regions indicates that average shear velocities at depths between 30 and 110 km increase rapidly with age. This increase occurs mainly because the depth to the base of the lithosphere increases; however, the shear velocities of the lithosphere also increase for the regions out to 100 Myr in age. Slightly lower velocities in the upper part of the lithosphere for greater ages may be due to a large influx of mid-plate volcanism during the Cretaceous.

Separate inversions of Love- and Rayleigh-wave velocities indicate that polarization anisotropy can be resolved for the lithosphere. Polarization anisotropy cannot be resolved for the low-velocity zone beneath the Pacific

* Now at the Department of Geophysics, National Central University, Chung-Li, Taiwan 320, Republic of China.

using these data, except possibly in the youngest regions, where lateral complexities of the East Pacific Rise are apt to affect the data adversely. Assuming that we can adequately invert our Love- and Rayleigh-wave data separately to obtain information on anisotropy, we find that average *SV* velocities in the lithosphere increase from about 4.3 to 4.6 km/s, and average *SH* velocities increase from about 4.5 to 4.7 km/s, from the youngest to oldest regions. Average velocities in the upper portion of the low-velocity zone increase from about 4.1 to about 4.25 km/s for the same regions.

The existence of anisotropy in the lithosphere is constant with the results of seismic refraction experiments in the Pacific and supports periodite as the predominant upper mantle material. The occurrence of anisotropy throughout the entire lithosphere, suggests a situation in which periodite crystallizes at the base of the lithosphere from a partially molten low-velocity zone and olivine crystals become aligned in response to the stress field within the Pacific plate.

Introduction

Studies of the dispersion of seismic surface waves have made important contributions to our understanding of the properties of the upper mantle beneath the Pacific (e.g. Ewing & Press 1952; Oliver, Ewing & Press 1955; Dorman, Ewing & Oliver 1960; Aki & Press 1961; Saito & Takeuchi 1966; Piermattei & Nowroozi 1969; Leeds, Knopoff & Kausel 1974; Yoshii 1975; Forsyth 1975b; Schlue & Knopoff 1977). Several of these studies concentrated only on Rayleigh-wave measurements. The use of Love waves for periods less than 100 s had until recently been largely abandoned because of the possibility of higher-mode interference (Thatcher & Brune 1969). However, if they can be obtained reliably, Love-wave velocities should provide additional information which cannot be obtained from Rayleigh wave measurements alone.

It is well known that group- and phase-velocity dispersion curves contribute generally the same information about a structural model (Bloch, Hales & Landisman 1969; Der, Masse & Landisman 1970; Wiggins 1972). The group velocities are useful, however, because they are more sensitive to detailed changes in elastic properties than are phase velocities. It is important, in addition, to have phase velocity information since group velocities are subject to an additional degree of non-uniqueness over phase velocities (Pilant & Knopoff 1970). By studying both group and phase velocities of Rayleigh and Love waves, we hope to obtain more detailed shear velocity models of the Pacific crust and upper mantle than are presently available, and also to infer the degree of anisotropy required in these models with greater precision than is now possible.

During this study, the attenuation data obtained by Mitchell, Yacoub & Correig (1977) will be used to correct the observed group and phase velocities for the effects of anelasticity. The stochastic form of the Backus–Gilbert inversion technique (Der *et al.* 1970; Franklin 1970; Jordan & Franklin 1971; Wiggins 1972) will be applied to derive shear velocity models for the Pacific mantle.

Data selection and processing

EARTHQUAKES AND SEISMOGRAPH STATION SELECTION

Twelve shallow, moderate size earthquakes (focal depths less than 40 km, magnitudes between 5.0 and 6.3) with epicentres around the Pacific, were chosen as the sources in this

Table 1. Earthquakes used in this study.

Event	Date	Origin time	Latitude	Longitude	Depth (km)	*P* axis		*T* axis	
		h m s	(°)	(°)		Trend	Plunge	Trend	Plunge
1	1963 April 3	14 47 50.4	55.35 S	128.24 W	4.5	248	32	350	9
2	1967 January 21	02 54 00.4	49.71 S	114.90 W	5	63	5	152	5
3	1963 March 7	05 21 59.6	26.87 S	113.58 W	8	154	11	244	0
4	1967 April 1	10 41 00.2	4.59 S	105.81 W	5	58	0	148	0
5	1965 December 6	11 34 48.9	18.90 N	107.20 W	5	157	3	67	3
6	1964 July 5	19 07 58.2	26.26 N	110.22 W	28	176	0	86	0
7	1966 August 7	17 36 22.8	31.72 N	114.42 W	5	125	0	35	0
8	1966 August 7	02 13 04.7	50.60 N	171.20 W	39	43	62	168	18
9	1965 July 29	08 29 21.2	50.90 N	171.40 W	23	106	62	355	10
10	1965 October 1	08 52 04.4	50.10 N	178.20 E	23	292	65	197	0
11	1969 August 14	14 19 01.6	43.10 N	147.50 E	33	167	58	336	32
12	1966 February 10	14 21 11.2	20.77 N	146.38 E	38	131	10	224	20

References:

These fault-plane solutions were obtained by Forsyth (1975b), 2, 3, 4; Sykes (1967), 1, 5; Sykes (1970), 6, 7; Stauder (1968a, b), 8, 9, 10; Stauder & Mualchin (1976), 11; Katsumada & Sykes (1969), 12; respectively.

study. The focal mechanisms of these earthquakes were given in previous studies (Sykes 1967, 1970; Stauder 1968a, b; Katsumada & Sykes 1969; Forsyth 1975b; Stauder & Mualchin 1976). The solution of event 7 (Sykes 1970) was modified slightly to be consistent with *P*-wave first motions at the stations GUA and RAB. Detailed information about the earthquake fault-plane solutions is given in Table 1. In order to obtain the best possible dispersion data set, we chose those stations for which the propagation paths of the surface waves were entirely or predominantly (more than 95 per cent) within the Pacific plate. This selection minimizes the adverse effects which arise from crossing plate boundaries or from passing through the continental margins. All of the selected stations belong to the World-Wide Standard Seismograph Network and are located in or around the Pacific plate (Fig. 1).

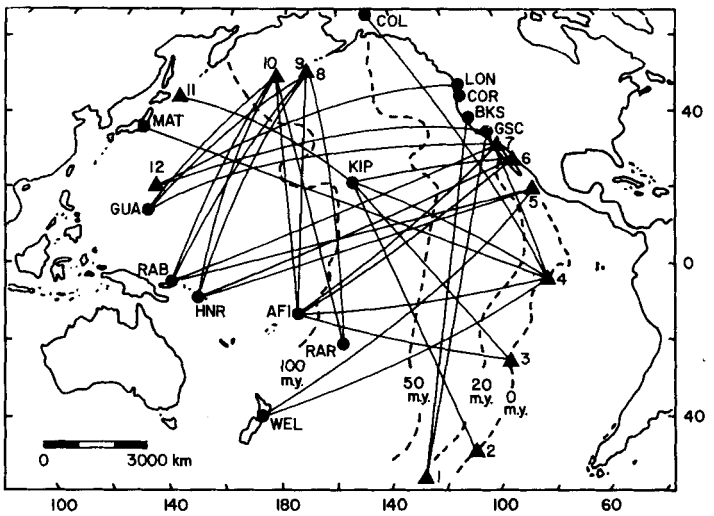

Figure 1. Map of the Pacific showing events, stations and propagation paths for Rayleigh waves. The same paths are used for Love waves except that paths 4-WEL, 9-AFI, 9-RAR, 10-HNR and 11-COR are not included. The dashed lines denote isochrons of 0, 20, 50 and 100 Myr in age.

GROUP AND PHASE VELOCITY DETERMINATIONS

The long-period seismograph records for the paths shown in Fig. 1 were digitized at a regular time interval of 2.0 s. The length of the digitized record depends on the dispersive character of the seismogram and the epicentral distance. To minimize possible errors which might be produced by a low signal/noise ratio, we have rejected all paths within 15° in azimuth from a node in the amplitude radiation pattern. Thirty-three Rayleigh- and 30 Love-wave paths were analysed in this study (Fig. 1). The group velocities of Rayleigh waves at periods between 16 and 110 s, and for Love waves at periods between 30 and 100 s, were determined by the multiple-filter method (Dziewonski, Bloch & Landisman 1969). The smaller period range for Love waves is due to possible higher-mode interference (Thatcher & Brune 1969). A filter of Gaussian shape and a window length which is four times the period of analysis were used in this study. The group velocity arrivals of the individual modes, using this filter, are usually sufficiently separated in time that their contribution to the filtered signals do not interfere. If the interfering signal was not sufficiently separated in time, the record, or portion of it, was rejected.

The phase velocities for each path at periods between 20 and 102.4 s for Rayleigh waves, and between 30 and 102.4 s for Love waves, were determined by the single-state method (Brune, Nafe & Oliver 1960). In using this method, the focal mechanism of the earthquake must be known and the time dependence of the displacement at the source is usually assumed to be a step function in time. Knowledge of these factors and an approximate knowledge of Earth structure in the Pacific region allow the calculation of the initial phase at the source. Examples of a few representative Rayleigh- and Love-wave group and phase

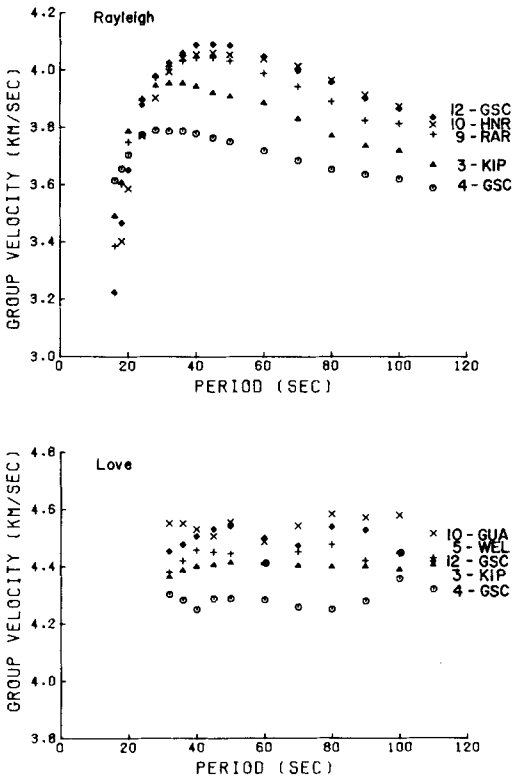

Figure 2. A few examples of observed Rayleigh- and Love-wave group velocity dispersion curves across the Pacific.

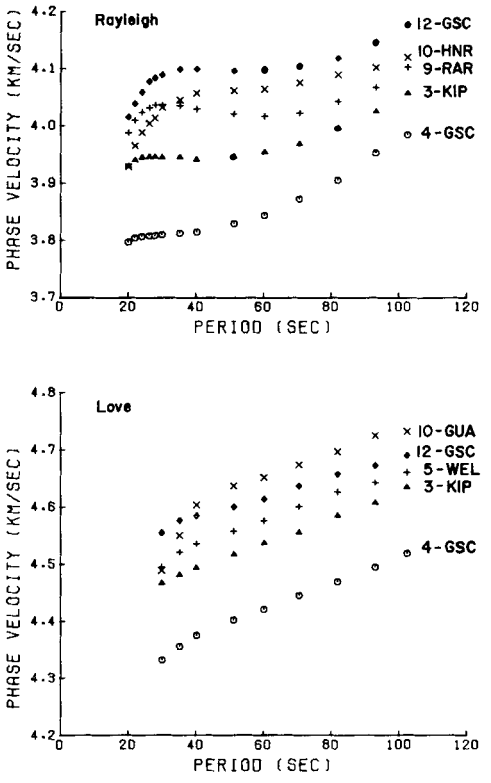

Figure 3. A few examples of observed Rayleigh- and Love-wave phase velocity dispersion curves across the Pacific.

velocity dispersion curves are shown in Figs 2 and 3. The group and phase velocities obtained from this study, for a few similar paths, are in good agreement with the results of previous studies (Kausel, Leeds & Knopoff 1974; Yoshii 1975; Schlue & Knopoff 1977).

The uncertainties to be expected in surface wave travel-times have been discussed by several authors (e.g. Forsyth 1975b; Yoshii 1975). These consist of time uncertainties associated with digitizing errors, inexact values for initial phase at the source, uncertainties in origin time and source location and effects of source finiteness. Forsyth (1975b) estimates the rms error arising from these effects to be about 5 s. Previous experience with continental dispersion studies has indicated to us that measured phases are adversely affected by noise and higher-mode interference. It is difficult to assess the extent of these effects, but we have taken a larger value of 8 s as the rms error in our phase travel-times. For our average path-length of about 8000 km and a velocity of 4.5 km/s (corresponding to Love waves), this leads to an uncertainty in phase velocities of about 0.02 km/s. The factors leading to errors in phase travel-times also contribute to errors in group travel-times. Larger errors are expected, however, because there is an inherent uncertainty in determining group velocities using the multiple-filter method. Der *et al.* (1970) apply an uncertainty principle to group velocity measurements and note that the greatest uncertainties occur at long periods where the position of the crest of the amplitude maxima is broadest. We estimate that the rms error of our travel-time uncertainties for group velocity measurements, including this additional factor, is about 12 s in the worst case. This time uncertainty leads to a group velocity uncertainty of about 0.03 km/s.

Regional changes and azimuthal variation

Recently, a series of studies based on phase or group velocities of Rayleigh waves across the Pacific have found that there are clear regional changes associated with the age of the ocean floor (Kausel *et al.* 1974; Yoshii 1975; Forsyth 1975a, b). It also appears that both phase and group velocities of Rayleigh and Love waves have directional dependence (Forsyth 1975a, b). Therefore, the possibility of both regional velocity variations and azimuthal anisotropy are considered in this study.

In order to detect the regional changes in group and phase velocities of Rayleigh and Love waves, we have divided the Pacific into four regions of differing age (Fig. 1). The boundaries of the regions are chosen to correspond to isochrons of 20, 50 and 100 Myr as inferred from geomagnetic lineations (Kausel *et al.* 1974; Yoshii 1975). The decision to use only four regions is somewhat arbitrary. It was made partly to keep the number of inversion computer runs within reasonable limits (our regionalization required a minimum of 12 inversions using between 20 and 40 min each), and partly because our data set, as well as geological data (Winterer 1976), suggest that a regionalization based only upon lithospheric age may be oversimplified. We have, therefore, used a coarser regionalization than that used by some other authors reporting results for the Pacific.

In addition to regional changes, there may be an azimuthal variation of velocities due to anisotropy of the medium. Smith & Dahlen (1973) have shown that in a slightly anisotropic medium, the azimuthal variation of group and phase velocities for Rayleigh waves has the form

$$V(\omega, \theta) = A_0(\omega) + A_2(\omega) \cos 2\theta + B_2(\omega) \sin 2\theta + A_4(\omega) \cos 4\theta + B_4(\omega) \sin 4\theta$$

where θ is the direction of the wave propagation path from the source to the recording station, as measured clockwise from north and ω is the angular frequency.

In order to obtain a better explanation for Rayleigh- and Love-wave group and phase velocities, the pure-path method, as described by Forsyth (1975b), was applied to four models with different combinations of regional changes and azimuthal anisotropy terms as described in Table 2. Model 1 considered only regional velocity changes, model 2 considered regional velocity changes and 2θ terms for uniform anisotropy throughout the Pacific, model 3 considered velocity changes and 4θ, as well as 2θ, terms of anisotropy throughout the Pacific, and model 4 considered regional velocity changes as well as regional changes in the 2θ terms of anisotropy. By comparing the root mean square (rms) delay time residual

Table 2. Rms delay time residual errors for Rayleigh and Love waves at a period of 50 s.

Model	Description	Rms errors			
		Rayleigh waves		Love waves	
		Group velocity (s)	Phase velocity (s)	Group velocity (s)	Phase velocity (s)
1	Only regional changes in four regions	20.4	17.9	19.2	12.8
2	Regional changes in four regions and 2θ terms of uniform anisotropy throughout the entire Pacific	16.4	13.9	16.9	12.1
3	Regional changes in four regions and all of the four terms of uniform anisotropy throughout the entire Pacific	16.2	13.2	16.3	11.6
4	Regional changes in four regions and 2θ terms of different anisotropy in each region	14.2	11.0	14.2	10.3

errors computed from each model, the results show that residual errors are substantially improved if azimuthal anisotropy terms are taken into account. However, nearly the same rms errors occur for models 2 and 3, indicating that the coefficients of 4θ terms are small compared to those of the 2θ terms, and can be neglected.

An attempt was made with model 4 to derive the regionalized velocities when the degree of azimuthal anisotropy is assumed to be different in each region. The results in Table 2 show that an average improvement of about 2 s in the rms residual error has occurred as compared to model 2. This improvement is undoubtedly statistically significant; however, an inspection of the resulting regionalized velocities for regions 2, 3 and 4 indicate that the velocity differences between models 2 and 4 are usually less than 0.02 km/s and almost always less than 0.03 km/s. Greater differences, occasionally as much as 0.1 km/s, occur between the two models for region 1. Since we are primarily interested in the older regions of the Pacific, where the velocity differences between the two models are not great, we have elected to use the results of model 2, which assumes uniform anisotropy throughout the entire Pacific, for our inversion attempts. This assumption overlooks any effects due to reported changes in spreading direction in the Pacific (e.g. Molnar *et al.* 1975).

Because of our fairly coarse regionalization, the rms errors which result when our observed travel times are compared with theoretical times predicted by our models are larger than those reported by other authors. For instance, Forsyth (1975a, b) reports errors of 7.6 s for Rayleigh wave phase travel times at a period of 40 s, after dividing the eastern Pacific into two regions. The selected regionalization in the present study yields an rms residual error of 13.7 s for Rayleigh wave phase travel times at the same period. This value is substantially larger than the value estimated for the uncertainty in our measurements (8 s) as discussed in the preceding section. This discrepancy could undoubtedly be reduced with a finer regionalization. For velocities between 4.0 and 4.5 km/s along a path length of 8000 km (average for the present study), the corresponding velocity error would, however, be about 0.03 km/s which is the estimated uncertainty of measurement in our group velocities. We used our regionalized velocities for model 2 and calculated the expected average velocities between every event and recording station and compared these values with our observed velocities. The phase velocities calculated from the regional values differed from the observed values by 0.02 km/s or less in more than half the cases, and by 0.03 km/s or less in about 70 per cent of the cases. The corresponding differences for group velocities were 0.03 and 0.04 km/s (for half and 70 per cent of the cases, respectively). A few differences as large as 0.1 km/s occurred. The paths which exhibited the larger differences were usually associated with sources on the East Pacific Rise. For example, events 4 and 6 to stations KIP and AFI (see Fig. 1) can be cited as the worst cases. Observed velocities along paths between event 4 and stations KIP and AFI were lower than calculated values, and paths from event 6 to those stations were higher than calculated values. In addition, and to a lesser extent, observed velocities for the path from event 10 to AFI were lower than average and those for the path from event 10 to RAB were higher than average. Because of these results, we expect that any adverse effects of our coarse regionalization will be most severe for region 1(0–20 Myr). It is also likely that a further division of region 4, based upon geological information as well as sea-floor ages (as discussed in a later section) will provide more detailed information on that area.

The regionalized group and phase velocities of Rayleigh and Love waves and their standard deviations derived from model 2 are given in Tables 3 to 6, and are also shown in Figs 4 and 5. The azimuthal anisotropy coefficients and their uncertainties obtained from model 2 are shown in Figs 6 and 7. These results show that the regionalized Rayleigh wave group and phase velocities increase systematically with the age of the ocean floor and agree

Table 3. Regionalized Rayleigh-wave group velocities (km/s) derived from model 2.

Period (s)	Region 1	Region 2	Region 3	Region 4	Rms error (s)
16.0	3.696 ± 0.294	3.462 ± 0.075	3.379 ± 0.087		86.2
18.0	3.746 ± 0.189	3.697 ± 0.053	3.605 ± 0.059	3.270 ± 0.041	55.8
20.0	3.755 ± 0.095	3.755 ± 0.027	3.811 ± 0.033	3.544 ± 0.024	27.6
24.0	3.786 ± 0.061	3.843 ± 0.018	3.974 ± 0.022	3.771 ± 0.017	17.4
28.0	3.770 ± 0.064	3.890 ± 0.019	4.054 ± 0.025	3.894 ± 0.019	18.4
32.0	3.757 ± 0.055	3.910 ± 0.017	4.093 ± 0.022	3.965 ± 0.018	16.1
36.0	3.749 ± 0.058	3.901 ± 0.018	4.117 ± 0.023	4.010 ± 0.019	16.9
40.0	3.727 ± 0.056	3.885 ± 0.017	4.116 ± 0.023	4.044 ± 0.019	16.7
45.0	3.708 ± 0.052	3.862 ± 0.016	4.102 ± 0.021	4.066 ± 0.018	15.4
50.0	3.693 ± 0.054	3.830 ± 0.017	4.088 ± 0.022	4.070 ± 0.019	16.4
60.0	3.691 ± 0.053	3.777 ± 0.016	4.035 ± 0.021	4.055 ± 0.018	15.9
70.0	3.665 ± 0.055	3.727 ± 0.016	3.993 ± 0.022	4.007 ± 0.019	16.8
80.0	3.638 ± 0.058	3.694 ± 0.017	3.944 ± 0.023	3.956 ± 0.020	18.2
90.0	3.651 ± 0.054	3.679 ± 0.016	3.875 ± 0.020	3.918 ± 0.018	16.5
100.0	3.619 ± 0.061	3.643 ± 0.017	3.839 ± 0.023	3.892 ± 0.020	18.8
110.0	3.554 ± 0.079	3.628 ± 0.023	3.803 ± 0.030	3.865 ± 0.026	23.9

Table 4. Regionalized Rayleigh-wave phase velocities (km/s) derived from model 2.

Period (s)	Region 1	Region 2	Region 3	Region 4	Rms error (s)
20.0	3.784 ± 0.049	3.865 ± 0.015	4.024 ± 0.019	3.947 ± 0.015	14.0
22.0	3.776 ± 0.048	3.874 ± 0.015	4.053 ± 0.019	3.987 ± 0.015	14.0
24.0	3.777 ± 0.048	3.877 ± 0.015	4.063 ± 0.019	4.015 ± 0.016	14.0
26.0	3.774 ± 0.050	3.877 ± 0.015	4.067 ± 0.019	4.031 ± 0.016	14.4
28.0	3.774 ± 0.050	3.876 ± 0.015	4.070 ± 0.019	4.041 ± 0.016	14.4
30.0	3.775 ± 0.049	3.874 ± 0.015	4.067 ± 0.019	4.051 ± 0.016	14.3
35.3	3.778 ± 0.048	3.868 ± 0.015	4.064 ± 0.019	4.065 ± 0.016	14.0
40.0	3.782 ± 0.048	3.863 ± 0.014	4.057 ± 0.018	4.072 ± 0.016	13.7
51.2	3.806 ± 0.049	3.863 ± 0.014	4.047 ± 0.018	4.076 ± 0.016	13.9
60.0	3.823 ± 0.047	3.874 ± 0.014	4.045 ± 0.018	4.079 ± 0.015	13.3
70.6	3.851 ± 0.048	3.892 ± 0.014	4.051 ± 0.018	4.083 ± 0.015	13.2
81.9	3.896 ± 0.045	3.925 ± 0.013	4.063 ± 0.016	4.098 ± 0.014	12.1
93.1	3.934 ± 0.045	3.959 ± 0.013	4.087 ± 0.016	4.121 ± 0.014	11.8
102.4	3.980 ± 0.047	3.990 ± 0.013	4.118 ± 0.017	4.141 ± 0.014	12.1

Table 5. Regionalized Love-wave group velocities (km/s) derived from model 2.

Period (s)	Region 1	Region 2	Region 3	Region 4	Rms error (s)
32.0	4.293 ± 0.074	4.305 ± 0.021	4.468 ± 0.034	4.423 ± 0.023	15.0
36.0	4.281 ± 0.072	4.284 ± 0.020	4.500 ± 0.033	4.434 ± 0.022	14.6
40.0	4.265 ± 0.088	4.275 ± 0.024	4.532 ± 0.042	4.428 ± 0.027	18.0
45.0	4.298 ± 0.087	4.289 ± 0.024	4.524 ± 0.041	4.456 ± 0.027	17.6
50.0	4.287 ± 0.083	4.316 ± 0.023	4.509 ± 0.039	4.482 ± 0.026	16.9
60.0	4.279 ± 0.085	4.342 ± 0.024	4.483 ± 0.039	4.490 ± 0.027	17.4
70.0	4.266 ± 0.086	4.314 ± 0.024	4.538 ± 0.041	4.484 ± 0.028	17.7
80.0	4.274 ± 0.085	4.310 ± 0.024	4.532 ± 0.040	4.458 ± 0.027	17.4
90.0	4.289 ± 0.104	4.296 ± 0.029	4.518 ± 0.049	4.494 ± 0.033	21.1
100.0	4.369 ± 0.121	4.272 ± 0.032	4.516 ± 0.054	4.508 ± 0.037	23.6
110.0	4.338 ± 0.105	4.264 ± 0.028	4.507 ± 0.047	4.492 ± 0.033	20.8

Table 6. Regionalized Love-wave phase velocities (km/s) derived from model 2.

Period (s)	Region 1	Region 2	Region 3	Region 4	Rms error (s)
30.0	4.368 ± 0.072	4.323 ± 0.020	4.600 ± 0.034	4.509 ± 0.023	14.0
35.3	4.390 ± 0.068	4.349 ± 0.018	4.611 ± 0.032	4.539 ± 0.022	13.1
40.0	4.396 ± 0.064	4.374 ± 0.017	4.620 ± 0.030	4.562 ± 0.021	12.3
51.2	4.429 ± 0.064	4.393 ± 0.017	4.644 ± 0.030	4.585 ± 0.020	12.1
60.0	4.448 ± 0.063	4.407 ± 0.017	4.673 ± 0.029	4.599 ± 0.020	11.9
70.6	4.473 ± 0.066	4.421 ± 0.018	4.703 ± 0.030	4.618 ± 0.021	12.2
81.9	4.493 ± 0.065	4.446 ± 0.018	4.728 ± 0.030	4.642 ± 0.021	12.0
93.1	4.518 ± 0.065	4.473 ± 0.018	4.747 ± 0.030	4.664 ± 0.021	11.9
102.4	4.546 ± 0.065	4.495 ± 0.017	4.773 ± 0.030	4.686 ± 0.021	11.6

with the results of Yoshii (1975) and Kausel *et al.* (1974). The only exceptions to this systematic velocity increase are the lower velocities at shorter periods in region 4 as compared to those of region 3. Since Kausel *et al.* (1974) have not derived the regionalized Rayleigh wave phase velocities, we cannot compare our results directly with theirs. For the younger regions (1 and 2), however, our values are slightly lower than those of Yoshii (1975), but they agree very well with the results of Forsyth (1975b) for zones of 0–10 Myr and > 10 Myr in the East Pacific. The Love-wave velocities do not increase in the same systematic way that was noted for the Rayleigh waves. The regionalized Love-wave group velocities are very similar for regions 1 and 2, and also for regions 3 and 4. The regionalized

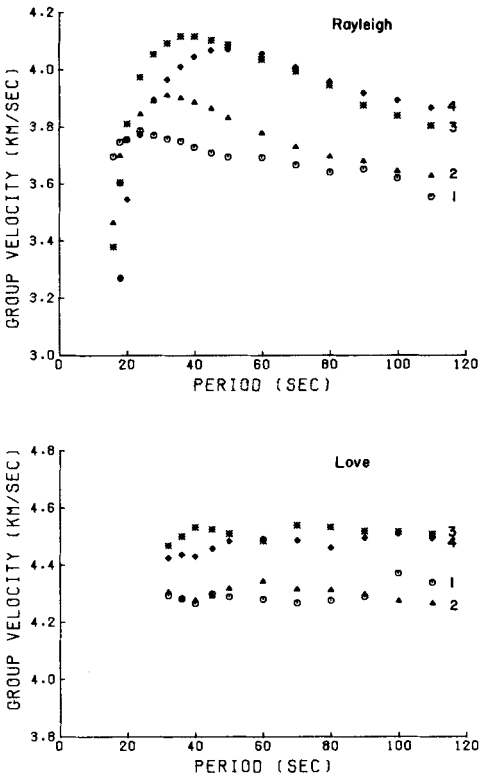

Figure 4. Regionalized Rayleigh- and Love-wave group velocities derived from model 2. The numbers denote regions 1 (0–20 Myr in age), 2 (20–50 Myr in age), 3 (50–100 Myr in age), and 4 (> 100 Myr in age).

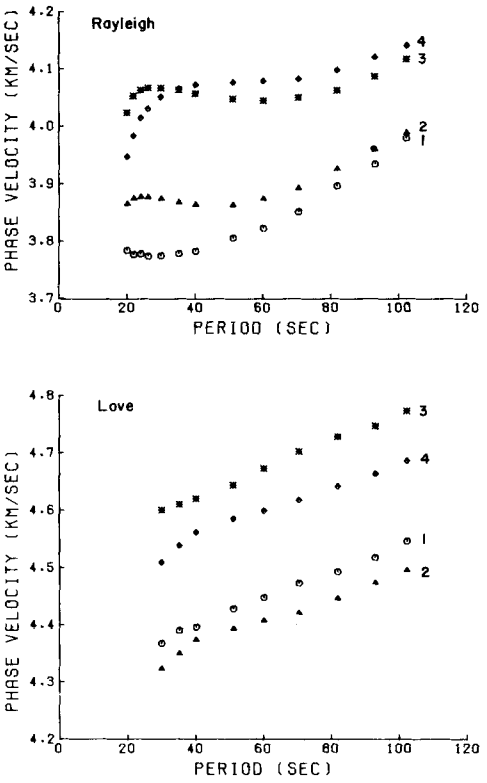

Figure 5. Regionalized Rayleigh- and Love-wave phase velocities derived from model 2. See the caption for Fig. 4 for an explanation of the meaning of the numbers.

Love-wave phase velocities in region 1 are higher than those in region 2, and the phase velocities in region 3 are higher than those in region 4.

The regionalized velocities over much of the observed period range increase with the age of the ocean floor, and the shift of the maximum group velocity of Rayleigh waves to longer periods in the older parts of the Pacific may be explained by a gradual thickening of the lithosphere (Leeds *et al.* 1974; Yoshii 1975; Forsyth 1975b). The fact that the regionalized group and phase velocities of Love waves are inconsistent with those predicted by models derived using only Rayleigh-wave velocities may require a structure which is anisotropic with respect to the polarization of shear waves (Forsyth 1975b; Schlue & Knopoff 1977). The regionalized group and phase velocities of the fundamental Rayleigh and Love modes obtained from model 2 will be used to derive regionalized structural models beneath the Pacific, after the effects of anelasticity have been corrected for as described in the next section.

Fig. 6 shows that the degree of azimuthal anisotropy is frequency-dependent, with the maximum anisotropy occurring in the period range from 28 to 60 s for Rayleigh-wave phase velocities and from 45 to 80 s for Rayleigh-wave group velocities. In this range, the values of A_2/A_0 are about -0.0070 for phase velocity and about -0.0073 for group velocity, the values of B_2/A_0 are about 0.0011 for phase velocity and about -0.006 for group velocity. These results indicate that a wave travelling in the direction of maximum velocity will be about 0.8 per cent faster than a wave travelling perpendicular to that direction. If it is assumed that the direction of maximum velocity is uniform throughout

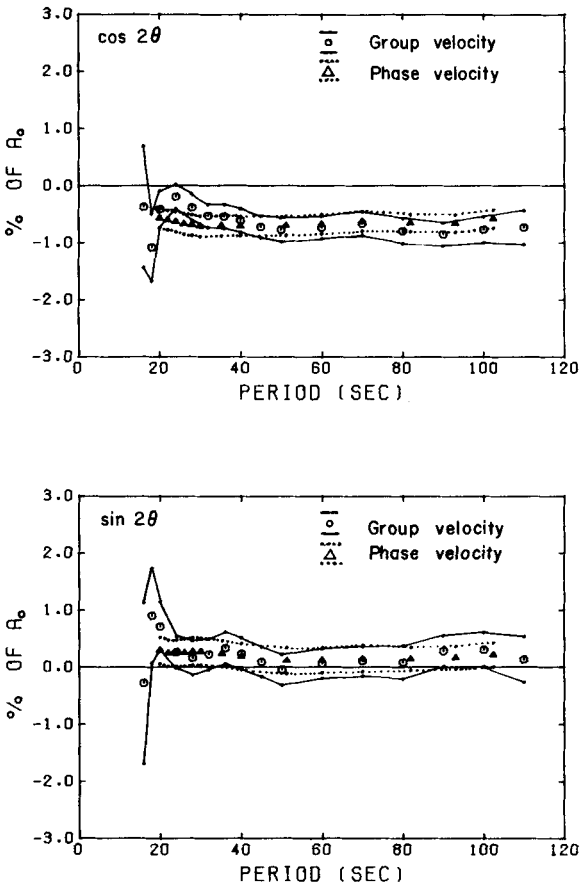

Figure 6. Azimuthal anisotropic coefficients and their uncertainty bands for Rayleigh waves derived using model 2.

the Pacific, that direction is 85° ± 6° as measured clockwise from the south. It is tempting to associate this direction with that of sea-floor spreading. The association, however, can be only a very coarse one, since changes in the direction of spreading in the Pacific are known to have occurred over the time interval included in this study (e.g. Molnar *et al.* 1975). Similar results are also obtained for Love-wave phase and group velocities (Fig. 7). These observations are in good agreement with seismic refraction measurements of *P*-wave velocities just beneath the Moho discontinuity obtained by Raitt *et al.* (1969) and Raitt *et al.* (1971). The agreement between surface wave observations and seismic refraction measurements, and the rough alignment with the spreading direction, suggest that there may be a common origin for these effects which is related either to the original formation of the lithosphere or to current tectonic processes associated with plate motions as described by Forsyth (1975b) in the eastern Pacific.

Anelasticity correction

It is usually assumed in seismic wave velocity studies that the Earth is perfectly elastic or that seismic frequencies are far from any absorption bands. However, the fact that seismic waves attenuate with distance show that the Earth is not an ideal elastic body. The effect

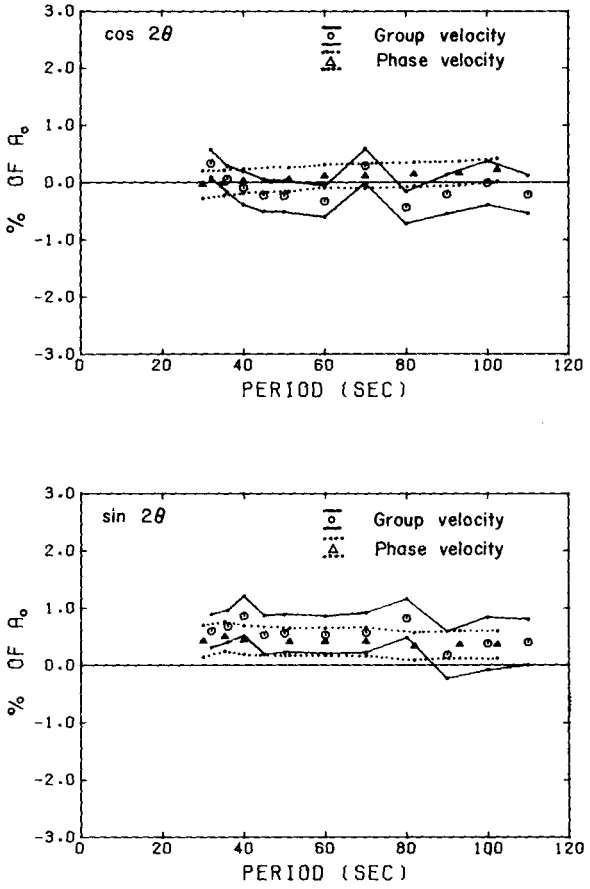

Figure 7. Azimuthal anisotropic coefficients and their uncertainty bands for Love waves derived using model 2.

and importance of surface wave phase velocity dispersion due to anelasticity have been discussed in recent studies (e.g. Liu *et al.* 1976; Kanamori & Anderson 1977). A correction of 0.5–1.5 per cent must be made for joint interpretation of surface wave and body wave data. When this correction is made, the discrepancy of the observed surface wave phase velocities and free oscillation periods from those predicted by the Jeffreys or Gutenberg model becomes much smaller than that which was previously found. This comparison clearly demonstrated the importance of physical dispersion in the inversion of surface wave and free oscillation studies.

The phase velocities of Rayleigh and Love waves at angular frequency ω computed for a structure defined at body wave frequencies can be corrected at each frequency by the following relations (Liu, Anderson & Kanamori 1976; Kanamori & Anderson 1977)

$$\Delta C_R(\omega) = C_R(\omega) \frac{1}{\pi Q_R(\omega)} \ln\left(\frac{\omega}{2\pi}\right)$$

and (1)

$$\Delta C_L(\omega) = C_L(\omega) \frac{1}{\pi Q_L(\omega)} \ln\left(\frac{\omega}{2\pi}\right)$$

where $Q_R(\omega)$ and $Q_L(\omega)$ are the observed Q values for Rayleigh and Love waves. These values can be calculated from

$$Q_R(\omega) = \frac{\pi}{\gamma_R(\omega) U_R(\omega) T}$$

$$Q_L(\omega) = \frac{\pi}{\gamma_L(\omega) U_L(\omega) T}$$

where $\gamma_R(\omega)$ and $\gamma_L(\omega)$ are the attenuation coefficients of Rayleigh and Love waves, $U_R(\omega)$ and $U_L(\omega)$ are the group velocities of Rayleigh and Love waves and T is the period. Recently, Mitchell *et al.* (1976) have determined a new set of fundamental Rayleigh- and Love-mode attenuation data pertaining to average Pacific crust and upper mantle. By inverting this new data set, a Q_β^{-1} model has been obtained by Mitchell (1976). The attenuation coefficients used for correcting the data of the present study are the theoretical values which were computed from the Q_β^{-1} model of Mitchell *et al.* (1977). In this study, these theoretical values are used to compute $Q_R(\omega)$ and $Q_L(\omega)$.

The effects of velocity dispersion arising from anelasticity can be corrected either in the theoretical velocity data for an earth model or in the observed data. In this study, the observed data which were obtained from model 2 were corrected to correspond to a perfectly elastic earth. Although there exist uncertainties in the observed velocity values, the contributions to the corrections from these uncertainties are very small and can be

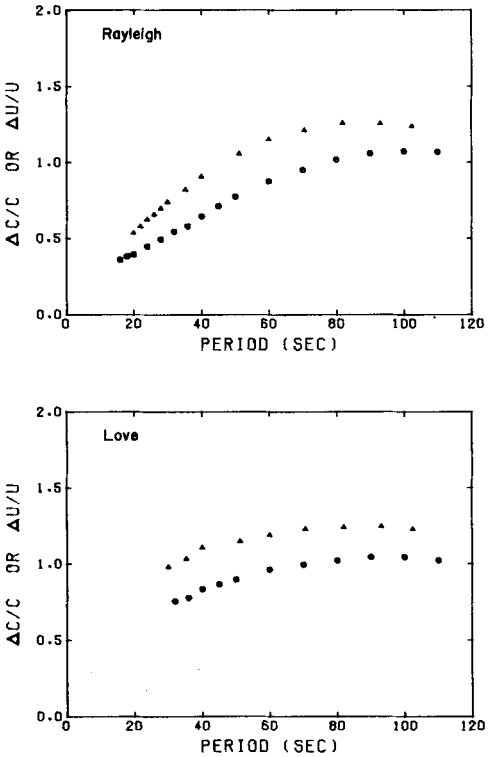

Figure 8. Percentage changes in Rayleigh- and Love-wave phase and group velocities due to anelasticity as a function of period derived for region 3. Triangles denote phase velocities and circles denote group velocities.

neglected. For an error of 0.03 km/s in the observed data, the maximum correction is 1.5 per cent and will produce an error of only 0.00045 km/s in the correction. Corrections for group velocities can be calculated from $\Delta C(\omega)$ by

$$\Delta U = \frac{U}{C}\left(2 - \frac{U}{C}\right)\Delta C + \left(\frac{U}{C}\right)^2 \omega \frac{d(\Delta C)}{d\omega}. \quad (2)$$

The phase and group velocities of Figs 4 and 5 and Tables 2–5 were all corrected appropriately using equations (1) or (2). An example of the fractional changes in Rayleigh- and Love-wave group and phase velocities as a function of period derived for region 3 (50–100 Myr) appears in Fig. 8.

Structural models from inversion

THE STARTING MODELS

The regionalized starting models, except for region 1, were based on the appropriate models of Leeds *et al.* (1974). In cases where those models did not explain our data, we adjust the velocities and/or depths to discontinuities until an approximate fit to the Rayleigh-wave velocities was achieved. For region 1, the group and phase velocities computed from the model of Forsyth (1975b) provide a better fit to the data of the present study than the

Table 7. Starting model parameters for region 1.

Layer	H(km)	D(km)	α(km/s)	β(km/s)	ρ(g cm^{-3})
1	3.4	1.7	1.52	0.0	1.03
2	1.4	4.1	5.15	3.0	2.6
3	4.7	7.15	6.8	3.9	2.9
4	5.0	12.0	7.9	4.4	3.4
5	5.0	17.0	7.9	4.4	3.4
6	5.0	22.0	7.9	4.4	3.4
7	5.5	27.25	7.9	4.4	3.4
8	6.0	33.0	7.6	4.1	3.4
9	7.0	39.5	7.6	4.1	3.4
10	7.0	46.5	7.6	4.1	3.4
11	10.0	55.0	7.6	4.1	3.4
12	10.0	65.0	7.6	4.1	3.4
13	10.0	75.0	7.6	4.1	3.4
14	10.0	85.0	7.6	4.1	3.4
15	10.0	95.0	7.6	4.1	3.4
16	10.0	105.0	7.6	4.1	3.4
17	10.0	115.0	7.6	4.1	3.4
18	15.0	127.5	7.6	4.1	3.4
19	15.0	142.5	7.6	4.1	3.4
20	25.0	162.5	7.9	4.35	3.4
21	25.0	187.5	7.9	4.35	3.4
22	25.0	212.5	7.9	4.35	3.4
23	25.0	237.5	7.9	4.35	3.4
24	33.0	266.5	8.2	4.55	3.5
25	33.0	299.5	8.2	4.55	3.5
26	34.0	333.0	8.2	4.55	3.5
27	50.0	375.0	9.32	5.19	3.76
28	50.0	425.0	9.32	5.19	3.76
29	50.0	475.0	9.8	5.4	3.96
30			9.8	5.4	3.96

model of Leeds *et al.* (1974) for that region. Forsyth's model was therefore used as the starting model for region 1. Since the thickness of each layer will be fixed in deriving the final models, the starting model should provide a reasonable fit to the data. For this reason, a layer with shear velocity 5.19 km/s was inserted in the subchannel at depths between about 350 and 450 km for the models obtained by Leeds *et al.* (1974) in order to fit the observed data at longer periods. The same crustal section was used throughout the entire Pacific for the inversion. The thickness of the water layer and sediment above the crustal section were varied, however, to be in accordance with published values. Generally, the starting models come very close to fitting the Rayleigh-wave data, but not the Love-wave data, because they are based upon Rayleigh-wave data only. The parameters of the starting models for the four regions are given in Tables 7 to 10.

INVERSION PROCEDURE AND SHEAR VELOCITY

Modern inversion theory (Backus & Gilbert 1970) in stochastic form as described by Franklin (1970), Jordan & Franklin (1971) and Wiggins (1972), has been applied to derive shear velocity models for four regions of differing age. The linear approximation reduces the problem to one of solving an under-determined set of linear equations for the first-order corrections to the starting model. The exact velocities are computed for the correct model, which is then used as a new starting model. The theoretical group and phase

Table 8. Starting model parameters for region 2.

Layer	H(km)	D(km)	α(km/s)	β(km/s)	ρ(g cm^{-3})
1	4.4	2.2	1.52	0.0	1.03
2	0.1	4.45	1.65	1.0	2.0
3	1.4	5.2	5.15	3.0	2.6
4	4.7	8.25	6.8	3.9	2.9
5	6.4	13.8	8.0	4.5	3.4
6	7.0	20.5	8.0	4.5	3.4
7	7.0	27.5	8.0	4.5	3.4
8	7.0	34.5	8.0	4.5	3.4
9	7.0	41.5	8.0	4.5	3.4
10	10.0	50.0	7.6	4.2	3.4
11	10.0	60.0	7.6	4.2	3.4
12	10.0	70.0	7.6	4.2	3.4
13	10.0	80.0	7.6	4.2	3.4
14	15.0	92.5	7.6	4.2	3.4
15	15.0	107.5	7.6	4.2	3.4
16	15.0	122.5	7.6	4.2	3.4
17	15.0	137.5	7.6	4.2	3.4
18	15.0	152.5	7.6	4.2	3.4
19	20.0	170.0	7.6	4.2	3.4
20	20.0	190.0	7.6	4.2	3.4
21	20.0	210.0	7.6	4.2	3.4
22	25.0	232.5	8.2	4.55	3.5
23	25.0	257.5	8.2	4.55	3.5
24	30.0	285.0	8.2	4.55	3.5
25	30.0	315.0	8.2	4.55	3.5
26	30.0	345.0	8.2	4.55	3.5
27	40.0	380.0	9.32	5.19	3.76
28	50.0	425.0	9.32	5.19	3.76
29	50.0	475.0	9.8	5.4	3.96
30			9.8	5.4	3.96

Table 9. Starting model parameters for region 3.

Layer	H(km)	D(km)	α(km/s)	β(km/s)	ρ(g cm^{-3})
1	4.7	2.35	1.52	0.0	1.03
2	0.2	4.8	1.65	1.0	2.0
3	1.4	5.6	5.15	3.0	2.6
4	4.7	8.65	6.8	3.9	2.9
5	8.0	15.0	8.1	4.6	3.4
6	8.0	23.0	8.1	4.6	3.4
7	9.0	31.5	8.1	4.6	3.4
8	9.0	4.05	8.1	4.6	3.4
9	9.0	49.5	8.1	4.6	3.4
10	9.0	58.5	8.1	4.6	3.4
11	9.0	67.5	8.1	4.6	3.4
12	9.0	76.5	8.1	4.6	3.4
13	9.0	85.5	8.1	4.6	3.4
14	15.0	97.5	7.6	4.16	3.4
15	15.0	112.5	7.6	4.16	3.4
16	15.0	127.5	7.6	4.16	3.4
17	15.0	142.5	7.6	4.16	3.4
18	15.0	157.5	7.6	4.16	3.4
19	15.0	172.5	7.6	4.16	3.4
20	20.0	190.0	8.2	4.55	3.5
21	20.0	210.0	8.2	4.55	3.5
22	30.0	235.0	8.2	4.55	3.5
23	30.0	265.0	8.2	4.55	3.5
24	30.0	295.0	8.2	4.55	3.5
25	30.0	325.0	8.2	4.55	3.5
26	30.0	355.0	8.2	4.55	3.5
27	40.0	390.0	9.32	5.19	3.76
28	40.0	430.0	9.32	5.19	3.76
29	50.0	475.0	9.8	5.4	3.96
30			9.8	5.4	3.96

velocities are calculated by the Haskell method (Haskell 1953) as modified by Harkrider (1964, 1970). A spherical earth correction has been made by the Biswas Earth Flattening formula (Biswas & Knopoff 1970; Schwab & Knopoff 1972; North & Dziewonski 1976) to the theoretical velocities. Partial derivatives of the group and phase velocities with respect to the parameters were calculated numerically by the ΔP (delta partial) method (Takeuchi, Dorman & Saito 1964; Rodi *et al.* 1975). Plots of the partial derivatives with respect to shear velocity are shown in Figs 9 and 10. For the period range considered in this study, the shear velocities have a much larger effect on the dispersion than either the density or the compressional velocity. As discussed by Bloch *et al.* (1969), the shear velocity partial derivatives have the following features: (1) increases (or decreases) in shear velocity cause only increases (or decreases) in phase velocity, whereas changes in shear velocity cause either increases or decreases in group velocity, depending on the depths at which the changes occur. It is, therefore, possible to increase (or decrease) the group velocity by increasing (or decreasing) the shear velocity at an appropriate depth or decreasing (or increasing) the shear velocity at some other depth in the model. (2) The Love-wave partial derivative curves, particularly for the upper layers, are broader than the corresponding Rayleigh-wave curves; the Rayleigh-wave curves have larger maxima. (3) Rayleigh waves at any period are influenced by the shear velocities at greater depths than Love waves for the corresponding periods.

Table 10. Starting model parameters for region 4.

Layer	H(km)	D(km)	α(km/s)	β(km/s)	ρ(g cm^{-3})
1	5.4	2.7	1.52	0.0	1.03
2	0.3	5.55	1.65	1.0	2.0
3	1.4	6.4	5.15	3.0	2.6
4	4.7	9.45	6.8	3.9	2.9
5	8.0	15.8	8.1	4.6	3.4
6	8.2	23.9	8.1	4.6	3.4
7	9.0	32.5	8.1	4.6	3.4
8	9.0	41.5	8.1	4.6	3.4
9	9.0	50.5	8.1	4.6	3.4
10	10.0	60.0	8.1	4.6	3.4
11	10.0	70.0	8.1	4.6	3.4
12	10.0	80.0	8.1	4.6	3.4
13	10.0	90.0	8.1	4.6	3.4
14	10.0	100.0	8.1	4.6	3.4
15	10.0	110.0	8.1	4.6	3.4
16	16.0	123.0	7.6	4.24	3.4
17	16.0	139.0	7.6	4.24	3.4
18	16.0	155.0	7.6	4.24	3.4
19	17.0	171.5	7.6	4.24	3.4
20	25.0	192.5	8.2	4.55	3.5
21	25.0	217.5	8.2	4.55	3.5
22	25.0	242.5	8.2	4.55	3.5
23	25.0	267.5	8.2	4.55	3.5
24	30.0	295.0	8.2	4.55	3.5
25	30.0	325.0	8.2	4.55	3.5
26	30.0	355.0	8.2	4.55	3.5
27	40.0	390.3	9.32	5.19	3.76
28	40.0	430.0	9.32	5.19	3.76
29	50.0	475.0	9.8	5.4	3.96
30			9.8	5.4	3.96

Although group- and phase-velocity dispersion curves contribute generally the same information about an earth model, the use of both group- and phase-velocity dispersion data is desirable in determining the earth model. Since the group velocity is a differential of the phase velocity, an infinite set of phase-velocity curves, and hence an infinite set of models, corresponds to any one group-velocity curve. For the same reason, however, small perturbations in phase velocity show up as larger variations in group velocity. Thus the group velocity dispersion, when inverted, should produce a more detailed earth model.

A computer program for general linear inversion of surface wave dispersion, written by W. L. Rodi, was used to derive the earth models in this study. Models are obtained iteratively until the rms error between the observed and theoretical data is satisfactorily small.

For surface wave dispersion, the shear velocity is the most important parameter in deriving the earth model; however, the density and compressional velocity changes (to a lesser extent) can also affect the Rayleigh-wave dispersion, especially if they occur at shallow depths. An attempt to invert both Love- and Rayleigh-wave velocities for all parameters (compressional velocity, shear velocity and density) simultaneously has been made. This inversion provides better values for the compressional velocity and density than were used in the starting model for the uppermost layers.

In this study, primary interest was in the shear velocity distribution in the Pacific upper

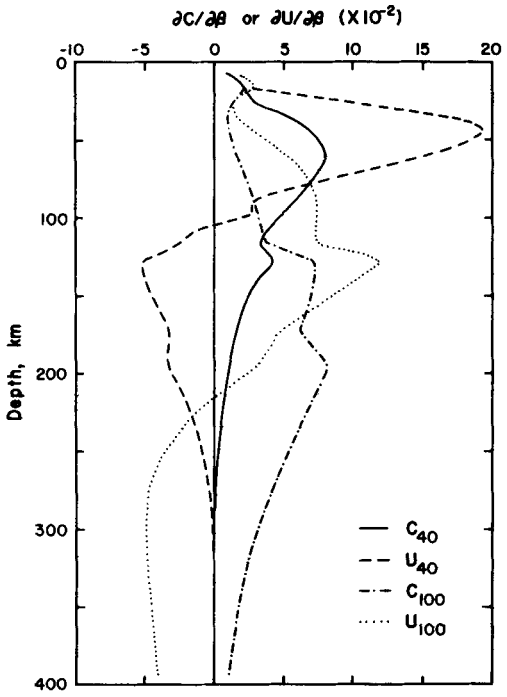

Figure 9. Rayleigh-wave phase (C) and group velocity (U) partial derivatives with respect to the shear velocity at periods 40 and 100 s.

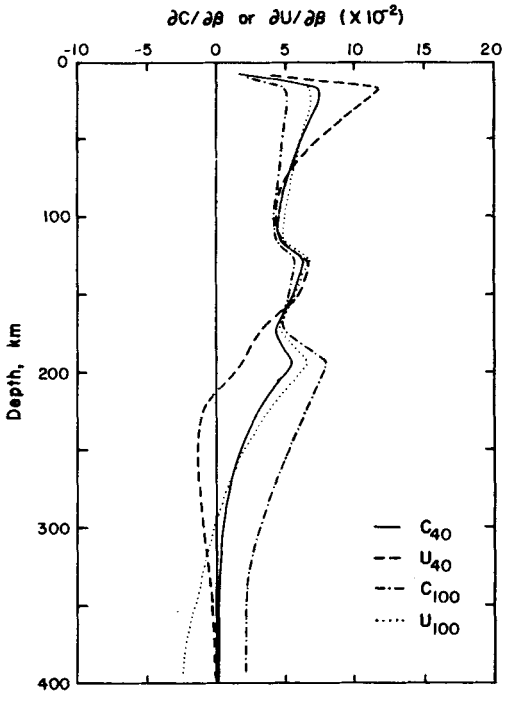

Figure 10. Love-wave phase (C) and group velocity (U) partial derivatives with respect to shear velocity at periods 40 and 100 s.

mantle, so that the following inversions were carried out by fixing the compressional velocity and density in each layer using the values obtained from the combined inversion for compressional velocity, shear velocity and density. From previous studies, we know that polarization anisotropy (*SH*-wave velocities which differ from *SV*-wave velocities) might exist in the upper mantle beneath the Pacific (Forsyth 1975b; Schlue & Knopoff 1977). Our approach to modelling our dispersion data will be to invert the regionalized Love- and Rayleigh-wave velocities both simultaneously and separately using isotropic inversion techniques in all cases. As shown by Crampin (1970), however, surface waves in layered structures containing anisotropic layers do not separate into independent families of Rayleigh and Love modes, but instead form a family of generalized modes having three-dimensional particle motion. For this reason, it is not generally valid to invert surface wave dispersion in anisotropic structures as if the structures were isotropic, but having different *SV* and *SH* velocities. This procedure is valid only for propagation in planes perpendicular to symmetry axes in transversely isotropic structures (Crampin 1976). If the Pacific lithosphere can be considered to be transversely isotropic with a horizontal symmetry axis perpendicular to the East Pacific Rise, then it is clear from Fig. 1 that a large fraction of our paths depart significantly from that desired propagation direction. Limitations of our models arising from this incomplete treatment of anisotropy will be discussed in the following section.

The final models for the four regions obtained from each inversion are plotted in Figs 11 to 14. The averaging kernels for each inversion are shown in Figs 15 to 18. Since the averaging kernels may be regarded as weighting functions through which we may view the general solution, the kernels are plotted versus depth at a few different depths.

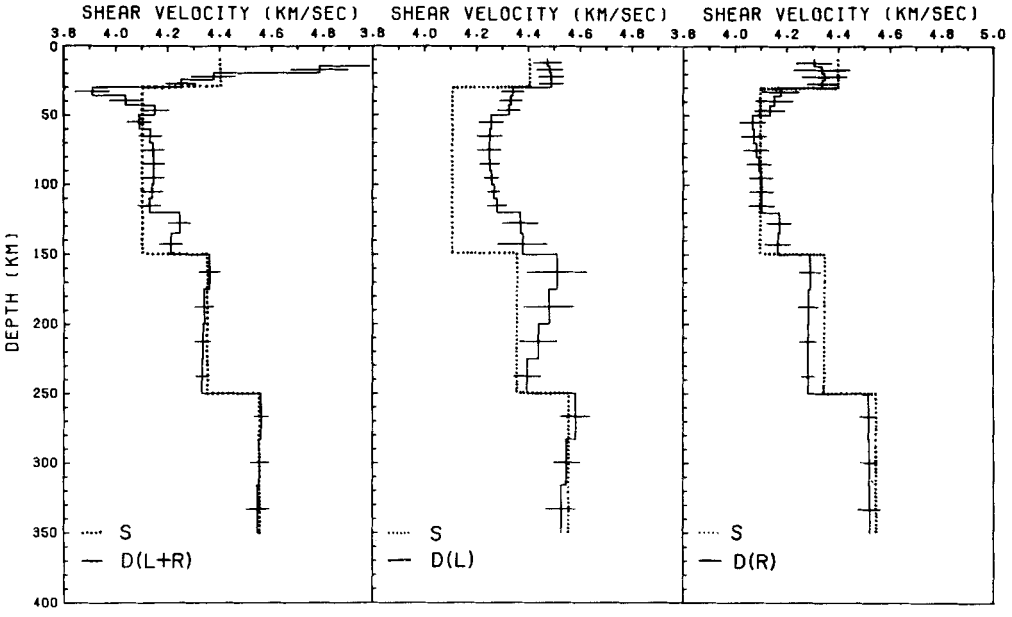

Figure 11. Shear velocity models and their standard deviations for region 1. S denotes the starting model, D(L + R) denotes the model derived from an inversion of the combined Love- and Rayleigh-wave data, D(L) denotes the model derived from an inversion of Love-wave data, and D(R) denotes the model derived from the inversion of Rayleigh-wave data.

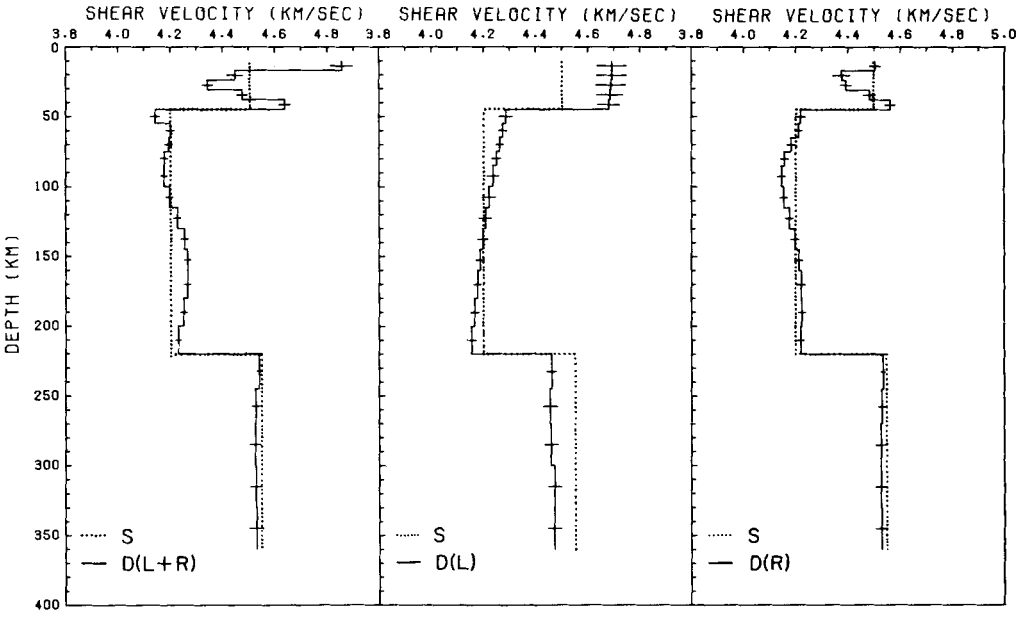

Figure 12. Shear velocity models and their standard deviations for region 2. See the caption for Fig. 11 for an explanation of the notation.

From Figs 19 to 22, it is clear that the stochastic inversion technique was successful in determining structural models from the observed data. At every period, nearly all of the values computed from the models which are derived from either simultaneous or separate inversion of Love- and Rayleigh-wave data are in good agreement with the observed data

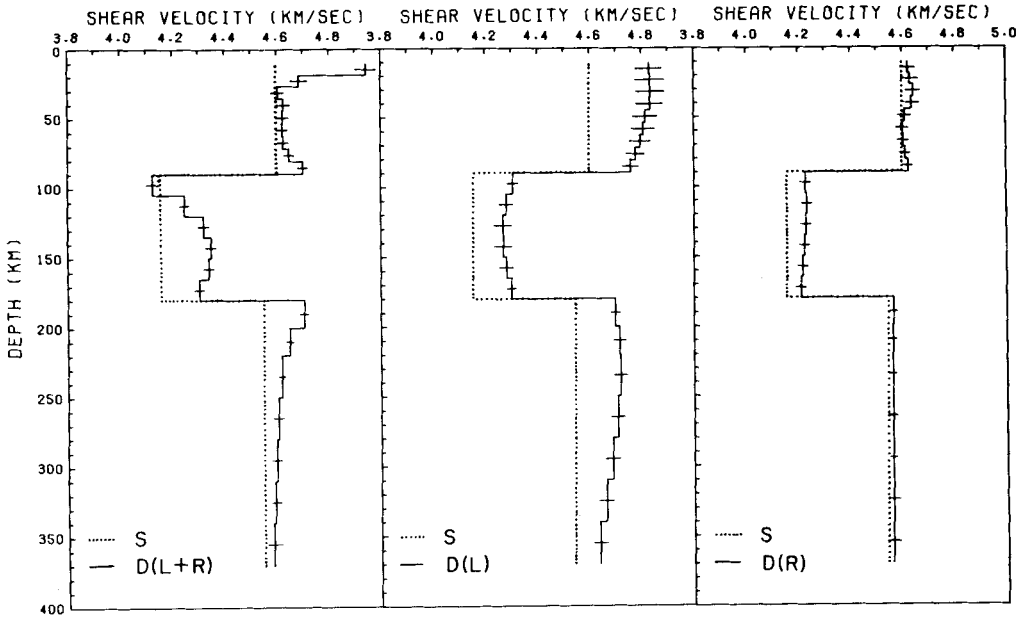

Figure 13. Shear velocity models and their standard deviations for region 3. See the caption for Fig. 11 for an explanation of the notation.

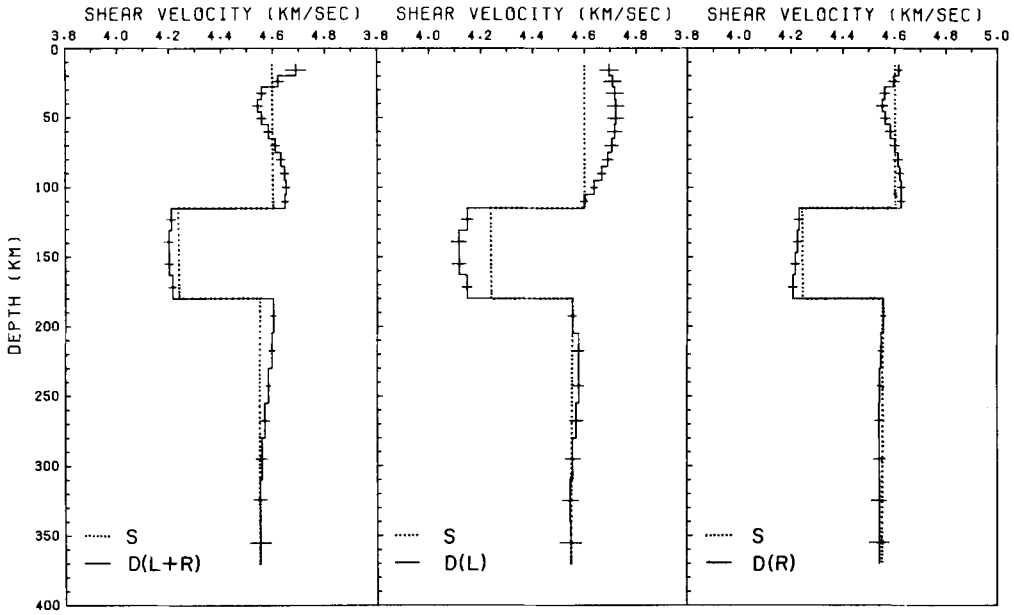

Figure 14. Shear velocity models and their standard deviations for region 4. See the caption for Fig. 11 for an explanation of the notation.

within one standard deviation. The standard deviation values for the surface wave data are approximately 0.06 km/s for region 1 and 0.02 km/s for other regions as discussed in the previous section.

The standard deviations estimated for the shear velocity models are generally less than 0.06 km/s in region 1 (0–20 Myr) and 0.03 km/s in other regions, if the Love- and Rayleigh-wave velocities are inverted simultaneously or only Rayleigh wave velocities are used. Slightly larger standard deviations for the models are obtained if the Love-wave velocities are inverted alone.

Figs 11 to 14 present shear velocity models for the four age regions obtained by inversions of (1) the combined Love- and Rayleigh-wave data, (2) the Love-wave data and

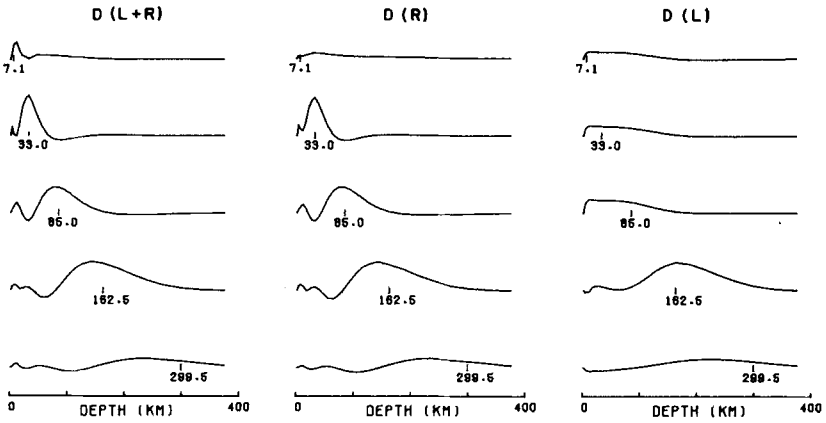

Figure 15. Averaging kernels for shear velocity perturbations in region 1 at various depths computed with the compressional velocity and density fixed.

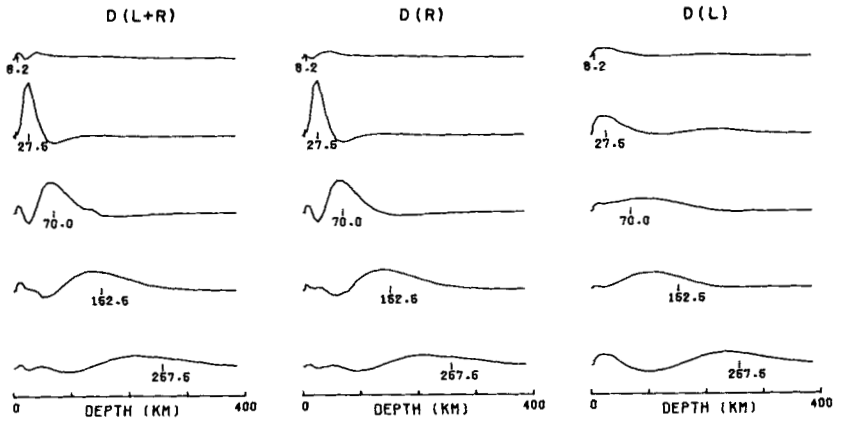

Figure 16. Averaging kernels for shear velocity perturbations in region 2 at various depths computed with the compressional velocity and density fixed.

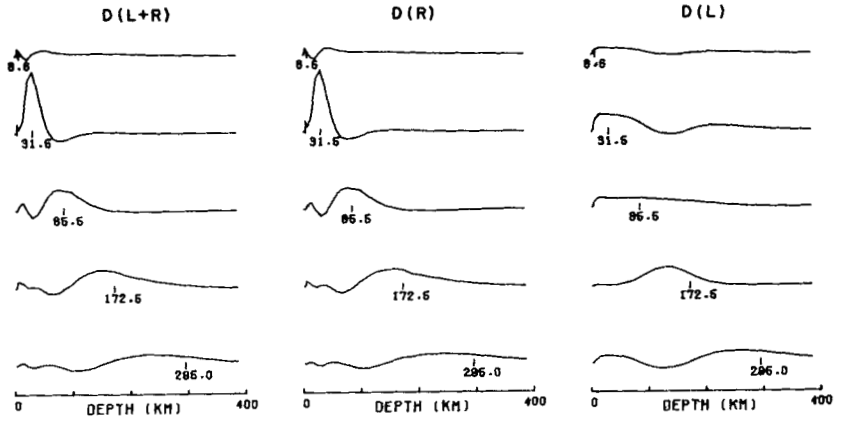

Figure 17. Averaging kernels for shear velocity perturbations in region 3 at various depths computed with the compressional velocity and density fixed.

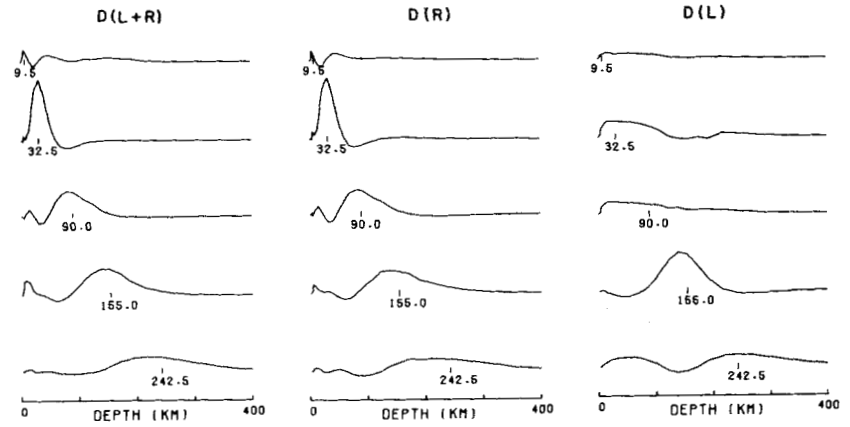

Figure 18. Averaging kernels for shear velocity perturbations in region 4 at various depths computed with the compressional velocity and density fixed.

(3) the Rayleigh-wave data. Data for the inversions consist of Rayleigh-wave group velocities at periods between 16 and 100 s, Rayleigh-wave phase velocities at periods between 20 and 100 s, Love-wave group velocities at periods between 32 and 100 s and love-wave phase velocities at periods between 32 and 100 s.

When assessing the models presented in this section, it is important also to consider the resolving kernels associated with various depth ranges for each model (Figs 15–18). The width of each kernel can be viewed as indicating the minimum thickness for any feature that can be resolved at a given depth. For instance, the Rayleigh kernel associated with a depth of 27.5 km in Fig. 16 suggests that a layer of 30–40 km thickness or greater can be resolved, whereas at 152.5 km depth the minimum thickness layer that can be resolved is about 150 km.

The models resulting from the combined inversion exhibit unrealistically high shear velocities in the uppermost mantle for all models except that of region 4. A way to avoid that difficulty, using the inversion method we have available, is to assume that polarization anisotropy (different *SV* and *SH* velocities) exists through some depth range and to invert the Love- and Rayleigh-wave data separately and obtain two different models for *SV* and *SH* waves. As discussed earlier, this procedure is not generally valid, however, and will yield reliable information only about larger-scale features. Detailed features of the models must not be accepted uncritically. We will describe the results of these inversions in the following paragraphs and discuss the more important features of the models, and their limitations in the following sections.

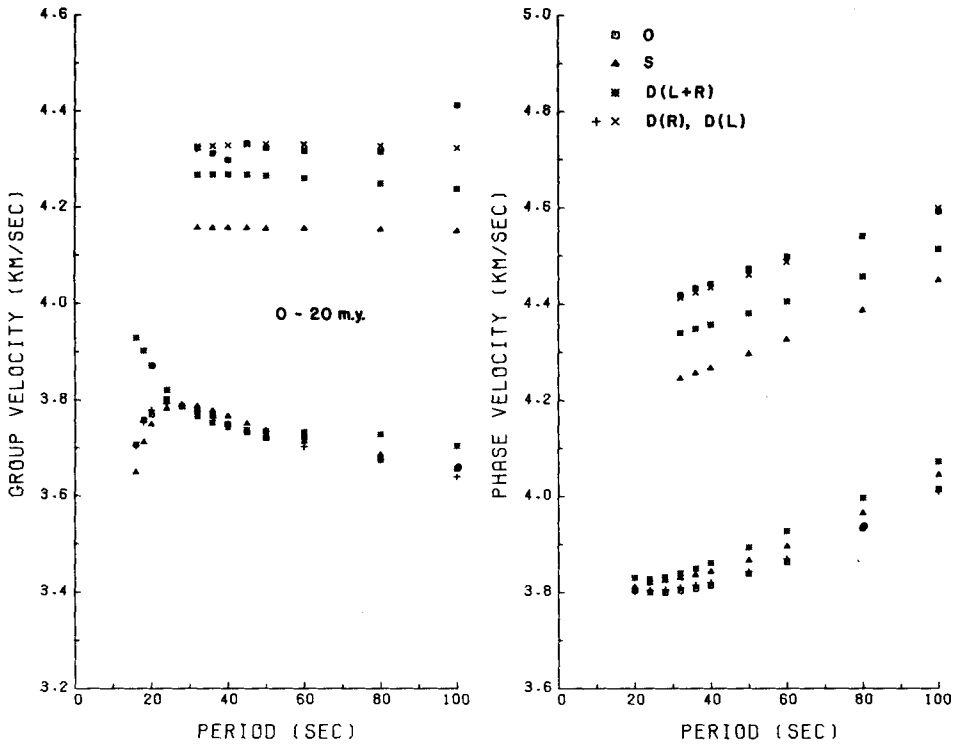

Figure 19. Regionalized group and phase velocities (O), and theoretical values computed from starting model (S) and derived models D(L + R), D(L) and D(R) for region 1.

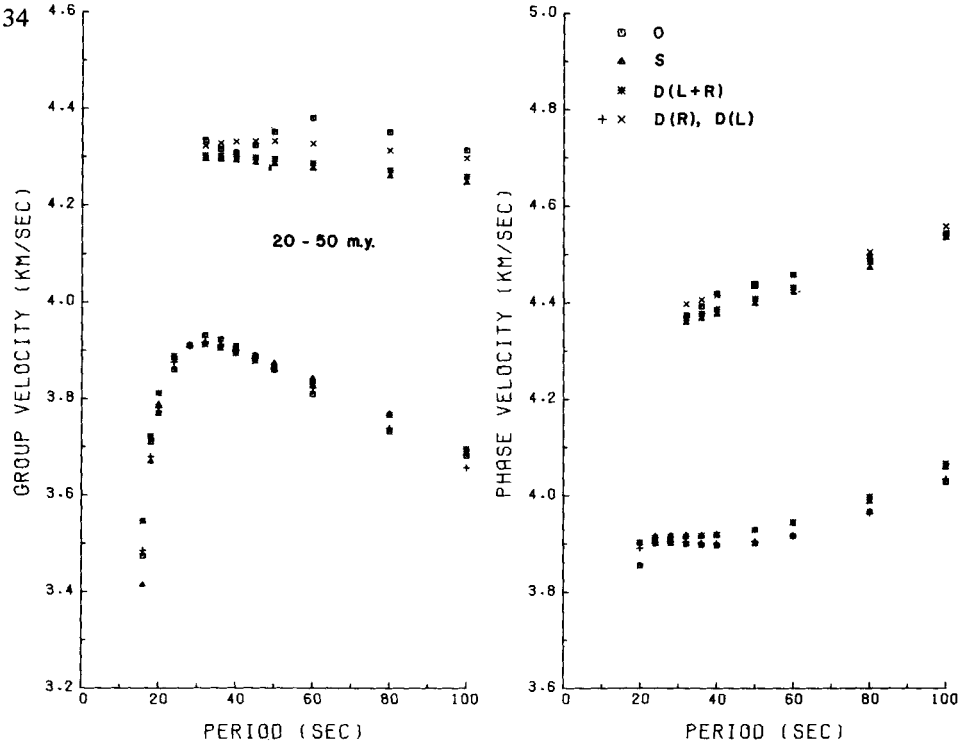

Figure 20. Regionalized group and phase velocities (O), and theoretical values computed from starting model (S) and derived models D(L + R), D(L) and D(R) for region 2.

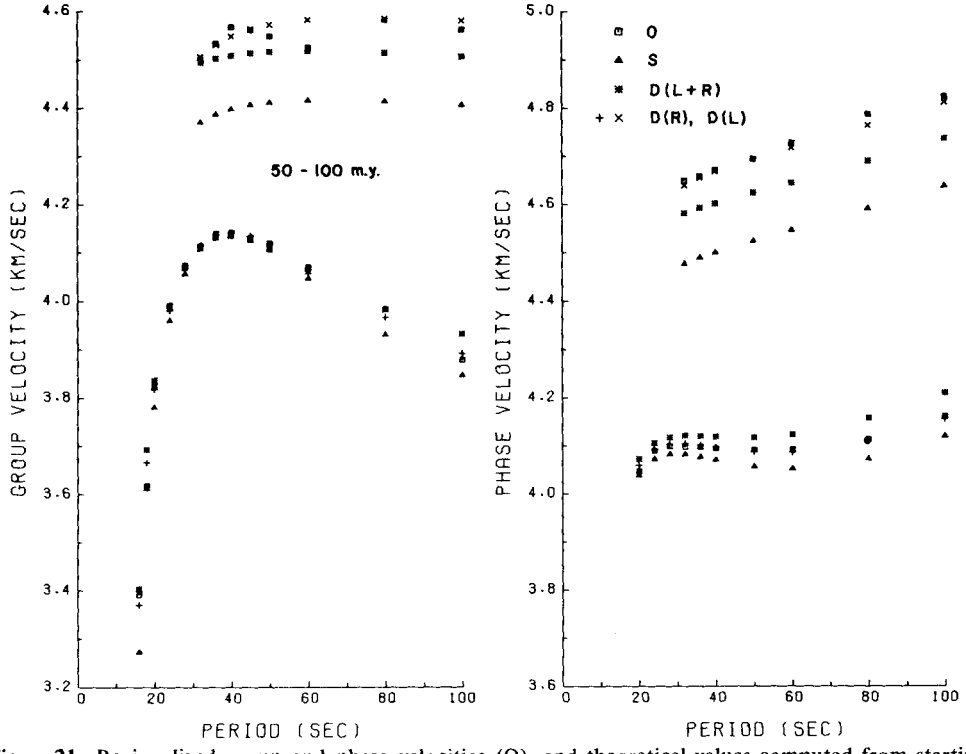

Figure 21. Regionalized group and phase velocities (O), and theoretical values computed from starting model (S) and derived models D(L + R), D(L) and D(R) for region 3.

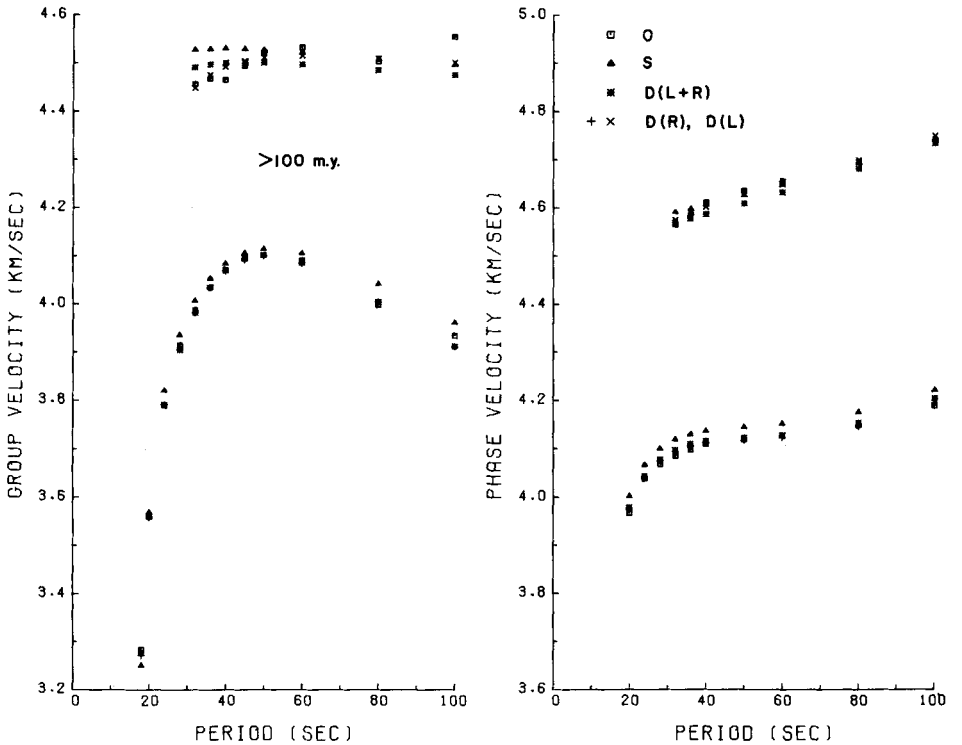

Figure 22. Regionalized group and phase velocities (O), and theoretical values computed from starting model (S) and derived models D(L + R), D(L) and D(R) for region 4.

The Rayleigh- and Love-wave models for region 1 (0–20 Myr) exhibit substantially different shear velocities at all depths between the surface and 250 km (Fig. 11). The *SH* velocities (from Love waves) are everywhere higher than the *SV* velocities (from Rayleigh waves). This effect is especially prominent in the low-velocity zone at depths between 30 and 150 km. The resolution of *SV* velocities is quite good in this depth range. Although the resolving power of Love waves is poor in that depth range, the low-velocity zone for *SH* is thick enough to be resolved. This region of the Pacific, however, is the only one for which substantial anisotropy can be resolved for the low-velocity zone. In view of this result, as well as the structural complexity that is likely to be associated with the East Pacific Rise, we tentatively propose that the anisotropy in the low-velocity zone suggested by the Love- and Rayleigh-wave models in Fig. 11 is only an apparent effect associated with lateral velocity variations in that region.

Region 2 (20–50 Myr) exhibits substantially different velocities for *SH* and *SV* in the lithosphere, the *SH* velocities being greater. However, *SH* and *SV* velocities in the low-velocity zone differ only slightly. The kernels in Fig. 16 indicate that the anisotropy in the lithosphere can be resolved. The broad Love-wave kernels at depths of 70 km and greater, however, indicate that it would be difficult to assign any significance to the small velocity differences in the low-velocity zones of the Love- and Rayleigh-wave models of Fig. 12.

The models of region 3 (50–100 Myr) again indicate substantially larger *SH* than *SV* velocities in the lithosphere (Fig. 13). The resolving kernels at a depth of 31.5 km suggest that this velocity difference is resolvable. The low-velocity zone again exhibits much smaller differences between *SH* and *SV* velocities, and the broad kernels (Fig. 17) at depths of 85.5 km and greater indicate that these small differences cannot be resolved.

The models of region 4 (> 100 Myr) also indicate that *SH* velocities are higher than *SV* in the lithosphere (Fig. 14). The low-velocity zone, on the other hand, exhibits higher velocities for *SV* than for *SH*. This result is the opposite of what most investigators observe when Rayleigh- and Love-wave velocities are incompatible. Inspection of the resolving kernels for this region (Fig. 18), however, indicates that the kernels are broader than the thickness of the low-velocity zone. It appears then that any differences between *SH* and *SV* for the low-velocity zone of this region of the Pacific cannot be resolved.

Figs 19–22 present the regionalized velocity values, and theoretical values for the starting model, the model derived from both Love- and Rayleigh-wave data, and models derived from Love and Rayleigh waves separately. In most cases, theoretical velocities for the starting models come close to fitting the Rayleigh-wave data, but sometimes differ from the Love-wave data by a great deal. This situation occurs because the starting models were derived using Rayleigh-wave data only.

It is clear from Fig. 19 that a reasonable model for region 1 (0–20 Myr) cannot be obtained from the combined inversion of both Love- and Rayleigh-wave data. Very good fits to the data can be achieved by fitting the Love- and Rayleigh-wave data separately. We suspect, however, that the good fits may be illusory, because we have assumed lateral uniformity of properties over a region which is probably very complex. For regions 2, 3 and 4 (20–50, 50–100, > 100 Myr, respectively) we can come closer to fitting all of the data with isotropic models. However, polarization anisotropy in the lithosphere, as suggested by separate inversions of the Love- and Rayleigh-wave data, lead to better agreement between theoretical velocities and observations in all cases.

Because of the relatively good resolution and small standard deviations for the models obtained from the inversion of Rayleigh-wave velocities alone, they are used to compare the features of the models for the four regions. Fig. 23 indicates that the lithosphere increases from an average thickness of about 30 km in region 1 to about 115 km throughout the region considered in this study. This result is consistent with results of Leeds *et al.* (1974), Schlue & Knopoff (1977) and Yoshii (1975).

Results of the present study indicate that *SV* velocities in the lithosphere increase from about 4.3 km/s to about 4.6 km/s through the first three regions (to about 100 Myr age) and then remain constant in its lower portion and even decrease slightly (to 4.56 km/s) at shallower depths in the oldest region. There are two factors which might be responsible for this apparent reduction in shear velocity in that region. A large outburst of mid-plate volcanism occurred during the Cretaceous period in the central Pacific (Winterer 1976). This extensive volume of volcanic rock is situated in the area of greatest path density of region 4. Another factor which might produce lower velocities in this region is the presence of a wedge of sediments near the trenches in the western Pacific. A few sources and stations are situated such that short path agreements will traverse trenches. The general pattern of increasing lithospheric shear velocities from younger to older regions supports the results of Forsyth (1977) and is consistent with the pattern of observed S_n velocities in the Pacific (Hart & Press 1975). Forsyth also observed a decrease of shear velocity with increasing depth within the lithosphere in a region of the Pacific which is between 100 and 135 Myr in age. Our results suggest the existence of a lithospheric low-velocity zone in the three oldest regions which we considered. This feature, however, cannot be clearly resolved and could result from systematic errors in our data or inadequacies in the isotropic inversion method. Further study will be necessary to verify, or to decide against, its existence.

Velocities within the upper portion of the upper mantle low-velocity zone also increase with increasing age of the Pacific sea floor. The small standard deviations and relatively narrow resolving kernels through this depth range indicate that this velocity increase is

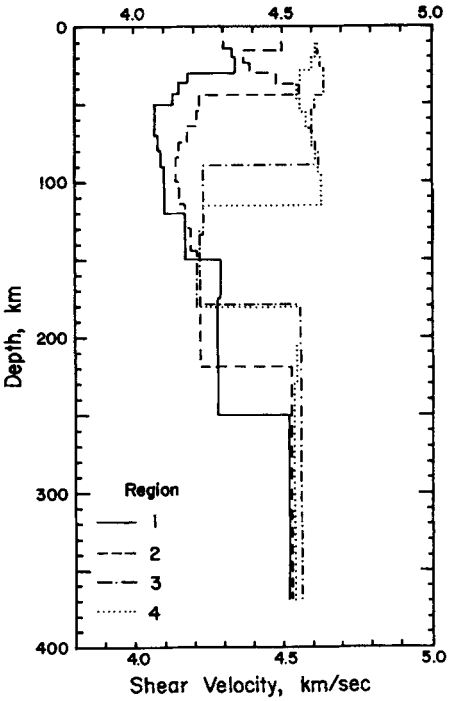

Figure 23. A comparison of the shear velocity models derived from the inversion of Rayleigh-wave velocities for the four regions in the Pacific.

resolvable if our isotropic inversion method is assumed valid, and again supports the result of Forsyth (1977). The central portion of the low-velocity zone exhibits no substantial changes. Because of the poor resolution at these depths, however, it is difficult to assign any certainty to this conclusion. For the same reason, the decrease in depth to the base of the low-velocity zone and the uniformity of shear velocity values at greater depths, as indicated by Fig. 23, must remain conjectural. Although there is some suggestion of anisotropy at depths below the low-velocity zone, the broad resolving kernels indicate that this possibility cannot be resolved.

Discussion

The combined Love- and Rayleigh-wave results of the present study support the conclusions of Schlue & Knopoff (1977) that polarization anisotropy, as well as systematic regional variations in shear velocity occur beneath the Pacific. We differ from those authors, however, in the depth interval through which we would place the anisotropy. The data of Schlue & Knopoff (1977) were not able to resolve any anisotropy for the lithosphere, but indicated a significant degree of anisotropy for the low-velocity zone. Our results, however, indicate that anisotropy occurs predominantly in the lithosphere, and is less pronounced, or absent, in the low-velocity zone.

At least three reasons could be responsible for this difference in results. First, the use of group velocities, in addition to phase velocities, in the present study permits us to resolve finer detail in the lithosphere than is possible using only phase velocities. Secondly, the

regionalizations used in the two studies are quite different. Our regionalization is much coarser than that of Schlue & Knopoff (1977), causing larger rms errors in our phase and group travel-times. Thirdly, the inversion procedures for the two studies differ considerably. Schlue & Knopoff (1977) solved for lid thickness (for four regions), *SV* and *SH* velocities in the lid, *SV* and *SH* velocities in the channel, density in the lid and density in the channel. By assuming that the velocities and densities for the lid and channel were uniform throughout the Pacific, they were able to restrict the number of unknown parameters to 10. The assumption of uniform lid properties, however, neglects the observations of Hart & Press (1975) which indicate an increase of S_n velocities with age. Schlue & Knopoff (1977) noted that the constraints used for this procedure might seem severe and alternate parameterizations might lead to significantly different results. The direct inversion of regionalized velocities, as used in the present study, permits much greater flexibility in the models which can be obtained. The assumption is made, however, that any lateral changes are gradual enough to be adequately approximated by a plane-layered structure.

It is important to discuss the limitations of our models which arise as a consequence of treating an anisotropic structure as if it were isotropic, but having different *SV* and *SH* velocities. As discussed earlier, in regions where anisotropy is present, this procedure, although widely used, is not generally valid. Crampin & King (1977) indicated that low-resolution data can be adequately modelled by using isotropic inversion techniques, but high-resolution results cannot be. Therefore, only the more major features of our derived models can be substantiated at the present time. We believe that these include the increase in thickness of, and velocity within the lithosphere, anisotropy within the lithosphere and the presence of a significant low-velocity zone. Because anisotropy is present in the lithosphere, and affects relatively short-period surface waves, it is difficult to obtain any detailed information regarding deeper portions of the upper mantle using isotropic inversion methods.

We consider that velocity anisotropy within the lithosphere is definitely indicated by our results. Knowledge of the depth interval over which velocity anisotropy occurs provides important information for inferring the nature of upper mantle material. The result of the present study, that anisotropy occurs throughout the lithosphere, strongly supports peridotite, as opposed to eclogite, as the major constituent of the lithosphere. The reason for this conclusion is that eclogite is not likely to possess significant anisotropy, even if it exhibits a strong mineral fabric (Kumazawa, Helmstaedt & Masaki 1971). Preferential alignment of olivine crystals, however, has often been suggested as a likely cause of anisotropy (e.g. Hess 1964). Since the entire lithosphere is anisotropic, the olivine crystals must be preferentially aligned as the lithosphere cools and thickens while moving away from the East Pacific Rise. The time of occurrence of the aligning process is presumably when peridotite solidifies at the base of the lithosphere from a partially molten low-velocity zone. The alignment is probably induced by the stress field responsible for the motion of the Pacific plate.

Conclusions

Clear, systematic variations in Rayleigh- and Love-wave phase and group velocities occur across the Pacific basin which correlate with the age of the sea floor. In support of the work of previous investigators, our results indicate that the lithosphere thickens with increasing age, and that velocities within the lithosphere also systematically increase with age. An exception to this pattern occurs in the shallow lithosphere of an older portion of the Pacific, where mid-plate volcanism or a wedge of trench sediments might cause a small velocity decrease compared with the next oldest region.

A small, but significant, degree of azimuthal anisotropy is associated with surface wave velocities in the Pacific. If it is taken to be uniform across the Pacific, the direction of maximum velocity is $85^\circ \pm 6^\circ$ and the anisotropy coefficient is less than 0.8 per cent.

Polarization anisotropy occurs in the lithosphere beneath the Pacific. Polarization anisotropy cannot be resolved for the low-velocity zone except in the young eastern Pacific. The apparent anisotropy in that region, however, may be due to lateral complexities associated with the East Pacific Rise. Velocities within at least the upper portion of the low-velocity zone may increase with increasing age of the sea floor. More detailed information concerning the properties of the upper mantle in the Pacific using surface waves will probably require inversion techniques which incorporate theoretical results of propagation in anisotropic media.

Acknowledgments

The authors are grateful to W. L. Rodi for providing us with a copy of his inversion program and for giving us much helpful advice on its use. R. B. Herrmann wrote the multiple-filter program for surface wave analysis. Leroy Dorman pointed out the occurrence of mid-plate volcanism in the central Pacific. This research was supported by the Division of Earth Sciences, National Science Foundation under Grant EAR 77-14482.

References

Aki, K. & Press, F., 1961. Upper mantle structure under oceans and continents from Rayleigh waves, *Geophys. J. R. astr. Soc.*, **5**, 292–305.

Backus, G. & Gilbert, F., 1970. Uniqueness in the inversion of gross earth data, *Phil. Trans. R. Soc. Lond. A*, **266**, 123–192.

Biswas, N. N. & Knopoff, L., 1970. An exact earth flattening correction for Love waves, *Bull. seism. Soc. Am.*, **60**, 1123–1127.

Bloch, S., Hales, A. L. & Landisman, M., 1969. Velocities in the crust and upper mantle of southern Africa from multi-mode surface wave dispersion, *Bull. seism. Soc. Am.*, **59**, 1599–1629.

Brune, J. N., Nafe, J. E. & Oliver, J., 1960. A simplified method for the analysis and synthesis of dispersed wave trains, *J. geophys. Res.*, **65**, 287–304.

Crampin, S., 1970. The dispersion of surface waves in multilayered anisotropic media, *Geophys. J. R. astr. Soc.*, **21**, 387–402.

Crampin, S., 1976. A comment on 'The early structural evolution and anisotropy of the oceanic upper mantle', *Geophys. J. R. astr. Soc.*, **46**, 193–197.

Crampin, S. & King, D. W., 1977. Evidence for anisotropy in the upper mantle beneath Eurasia from the polarization of higher mode seismic surface waves, *Geophys. J. R. astr. Soc.*, **49**, 59–85.

Der, Z., Masse, R. & Landisman, M., 1970. Effects of observational errors on the resolution of surface waves at intermediate distances, *J. geophys. Res.*, **75**, 3399–3409.

Dorman, J., Ewing, M. & Oliver, J., 1960. Study of shear velocity distribution in the upper mantle by mantle Rayleigh waves, *Bull. seism. Soc. Am.*, **50**, 87–115.

Dziewonski, A., Bloch, S. & Landisman, M., 1969. A technique for the analysis of transient seismic signals, *Bull. seism. Soc. Am.*, **59**, 427–444.

Ewing, M. & Press, F., 1952. Crustal structure and surface wave dispersion, Part II. Solomon Island earthquake of July 29, 1950, *Bull. seism. Soc. Am.*, **42**, 315–325.

Forsyth, D. W., 1975a. A new method for the analysis of multi-mode surface wave dispersion; application to Love-wave propagation in the east Pacific, *Bull. seism. Soc. Am.*, **65**, 323–342.

Forsyth, D. W., 1975b. The early structural evolution and anisotropy of the oceanic upper mantle, *Geophys. J. R. astr. Soc.*, **43**, 103–162.

Forsyth, D. W., 1977. The evolution of the upper mantle beneath mid-ocean ridges, *Tectonophys.*, **38**, 89–118.

Franklin, J. N., 1970. Well-posed stochastic extensions of ill-posed linear problems, *J. Math. Anal. Appl.*, **31**, 682–716.

Harkrider, D. G., 1964. Surface waves in multilayered elastic media, 1. Rayleigh and Love waves from buried sources in a multilayered elastic half-space, *Bull. seism. Soc. Am.*, **54**, 627–679.

Harkrider, D. G., 1970. Surface waves in multilayered elastic media, 2. Higher mode spectra and spectral ratios from point sources in plane layered earth models, *Bull. seism. Soc. Am.*, **60**, 1937–1967.

Hart, R. S. & Press, F., 1973. S_n velocities and the composition of the lithosphere in the regionalized Atlantic, *J. geophys. Res.*, **78**, 407–411.

Haskell, N. A., 1953. The dispersion of surface waves in multilayered media, *Bull. seism. Soc. Am.*, **43**, 17–34.

Hess, H., 1964. Seismic anisotropy of the uppermost mantle under the oceans, *Nature*, **203**, 629–631.

Jordan, T. H. & Franklin, J. N., 1971. Optimal solutions to a linear inverse problem in geophysics, *Proc. Nat. Acad. Sci.*, **68**, 291–293.

Kanamori, H. & Anderson, D. L., 1977. Importance of physical dispersion in surface wave and free oscillation problems: Review, *Rev. Geophys. Space Phys.*, **15**, 105–112.

Katsumada, M. & Sykes, L. R., 1969. Seismicity and tectonics of the western Pacific: Izu–Mariana–Caroline and Ryuku–Taiwan regions, *J. geophys. Res.*, **74**, 5923–5948.

Kausel, E. G., Leeds, A. R. & Knopoff, L., 1974. Variations of Rayleigh wave phase velocities across the Pacific Ocean, *Science*, **186**, 139–141.

Kumasawa, M., Helmstaedt, H. & Masaki, K., 1971. Elastic properties of eclogite xenoliths from diatremes of the East Colorado plateau and their implication to upper-mantle structure, *J. geophys. Res.*, **76**, 1231–1247.

Leeds, A. R., Knopoff, L. & Kausel, E. G., 1974. Variations of upper mantle structure under the Pacific Ocean, *Science*, **186**, 141–143.

Liu, H.-P., Anderson, D. L. & Kanamori, H., 1976. Velocity dispersion due to anelasticity: implications for seismology and mantle composition, *Geophys. J. R. astr. Soc.*, **47**, 41–58.

Mitchell, B. J., 1976. Anelasticity of the crust and upper mantle beneath the Pacific Ocean from the inversion of observed surface wave attenuation, *Geophys. J. R. astr. Soc.*, **46**, 521–533.

Mitchell, B. J., Leite, L. W. B., Yu, G.-K. & Herrmann, R. B., 1976. Attenuation of Love and Rayleigh waves across the Pacific at periods between 15 and 110 seconds, *Bull. seism. Soc. Am.*, **66**, 1189–1202.

Mitchell, B. J., Yacoub, N. & Correig, A., 1977. A summary of seismic surface wave attenuation and its regional variation across continents and oceans, Geophysical Monograph 20, *The Earth's Crust, its Nature and Physical Properties*, pp. 405–425, ed. Heacock, J., American Geophysical Union, Washington, DC.

Molnar, P., Atwater, T., Mammerickz, J. & Smith, S. M., 1975. Magnetic anomalies, bathymetry and the tectonic evolution of the South Pacific since the late Cretaceous, *Geophys. J. R. astr. Soc.*, **40**, 383–420.

North, R. G. & Dziewonski, A. M., 1976. A note on Rayleigh-wave flattening corrections, *Bull. seism. Soc. Am.*, **66**, 1873–1879.

Oliver, J., Ewing, M. & Press, F., 1955. Crustal structure and surface wave dispersion. Part IV. Atlantic and Pacific ocean basins, *Bull. Geol. Soc. Am.*, **66**, 913–946.

Piermattei, R. & Nowroozi, A., 1969. Dispersion of Rayleigh waves for purely oceanic paths in the Pacific, *Bull. seism. Soc. Am.*, **59**, 1905–1925.

Pilant, W. L. & Knopoff, L., 1970. Inversion of phase and group slowness dispersion, *J. geophys. Res.*, **75**, 2135–2136.

Raitt, R. W., Shor, G. G., Francis, T. J. C. & Morris, G. B., 1969. Anisotropy of Pacific upper mantle, *J. geophys. Res.*, **74**, 3095–3109.

Raitt, R. W., Shor, G. G., Morris, G. B. & Kirk, H. K., 1971. Mantle anisotropy in the Pacific Ocean, *Tectonophys.*, **12**, 173–186.

Rodi, W. L., Glover, P., Li, T. M. C. & Alexander, S. S., 1975. A fast, accurate method for computing group-velocity partial derivatives for Rayleigh and Love modes, *Bull. seism. Soc. Am.*, **65**, 1105–1114.

Saito, M. & Takeuchi, H., 1966. Surface waves across the Pacific, *Bull. seism. Soc. Am.*, **56**, 1067–1091.

Schlue, J. W. & Knopoff, L., 1977. Shear-wave polarization anisotropy in the Pacific basin, *Geophys. J. R. astr. Soc.*, **49**, 145–165.

Schwab, F. & Knopoff, L., 1972. Fast surface wave and free mode computations, in *Methods in Computational Physics*, **11**, 87–180, ed. Bolt, B. A., Academic Press, New York.

Smith, M. L. & Dahlen, F. A., 1973. The azimuthal dependence of Love and Rayleigh wave propagation in a slightly anisotropic medium, *J. geophys. Res.*, **78**, 3321–3333.

Stauder, W., 1968a. Mechanisms of the Rat Island earthquake sequence of February 4, 1965, with relation to the island arcs and sea-floor spreading, *J. geophys. Res.*, **73**, 3847–3858.

Stauder, W., 1968b. Tensional character of earthquake foci beneath the Aleutian trench with relation to sea-floor spreading, *J. geophys. Res.*, **73**, 7693–7701.

Stauder, W. & Maluchin, L., 1976. Fault motion in the larger earthquakes of the Kurile–Kamchatka Arc and of the Kurile–Hokkaido corner, *J. geophys. Res.*, **81**, 297–308.

Sykes, L. R., 1967. Mechanism of earthquakes and nature of faulting on mid-oceanic ridges, *J. geophys. Res.*, **72**, 2131–2153.

Sykes, L. R., 1970. Focal mechanism solution for earthquakes along the world rift system, *Bull. seism. Soc. Am.*, **60**, 1749–1752.

Takeuchi, H., Dorman, J. & Saito, M., 1964. Partial derivatives for surface wave phase velocity with respect to physical parameter changes within the earth, *J. geophys. Res.*, **69**, 3429–3441.

Thatcher, W. & Brune, J. N., 1969. Higher mode interference and observed anomalous apparent Love wave phase velocities, *J. geophys. Res.*, **74**, 6603–6611.

Wiggins, R. A., 1972. The general linear inverse problem: Implication of surface waves and free oscillations for earth structure, *Rev. Geophys. Space Phys.*, **10**, 251–285.

Winterer, E. L., 1976. Anomalies in the tectonic evolution of the Pacific, in Geophysical Monograph 19, *The Geophysics of the Pacific Ocean Basin and its Margin*, pp. 269–278, eds Sutton, G. H., Manghnani, M. L. & Moberly, R., American Geophysical Union, Washington, DC.

Yoshii, T., 1975. Regionality of group velocities of Rayleigh waves in the Pacific and thickening of the plate, *Earth planet. Sci. Lett.*, **25**, 305–312.